A Continuum Approximation for Particle Flux and Projectile Dynamics in Granular Impact

Michael Nicholas Petrakis

July 2026

1 Introduction

The interaction between a solid projectile and discrete granular matter is a problem in soft-matter physics with a wide range of applications, from planetary impact models to dynamic projectile penetration in marine sediments. When a spherical projectile enters a granular medium such as sand, its motion is governed by the coupled effects of projectile inertia, gravity, granular resistance, and the evolving geometry of the projectile–granular interface. Unlike a homogeneous fluid, a granular medium consists of discrete particles whose collective behavior can exhibit both fluid-like and solid-like characteristics depending on the applied stress and the local configuration of the grains. Therefore, standard hydrodynamic or aerodynamic drag laws are not sufficient on their own, requiring a new mathematical framework to describe the interactions.

Consider a spherical projectile released from an arbitrary height and colliding with a granular surface. During the collision, the projectile progressively becomes submerged within the granular medium, causing the region of interaction between the projectile and the granular surface to evolve with time. As the projectile moves, the changing intersection between its spherical surface and the granular boundary determines the portion of the projectile interacting with the medium. Therefore, the projectile dynamics and the geometric evolution of the submerged region cannot be treated as independent processes.

To address this, this paper develops a mathematical model for approximating this coupled interaction using multivariable vector calculus and continuum approximations. Instead of tracking millions of grains, the granular surface is represented by a three-dimensional Gaussian boundary function, providing a continuous and differentiable approximation of the granular surface. The projectile is represented as a time-dependent spherical surface, allowing the geometry of its intersection with the granular boundary to be described using spherical coordinates. A surface-flux formulation is then applied to construct a modeled particle-flux quantity linked to the submerged portion of the projectile.

The evolving intersection between the projectile and granular boundary is represented by an algebraic constraint involving the projectile position and the limiting submerged polar angle. Differentiating this constraint with respect to time creates a direct relationship between the projectile velocity and the rate of change of the submerged geometry. This relationship couples the projectile dynamics to the time evolution of the modeled particle-flux quantity. A quadratic continuum interaction model is later introduced to approximate the granular resistance acting on the submerged portion of the projectile, resulting in a coupled differential-algebraic equation system describing the projectile dynamics, granular resistance, and geometric interaction.

The mathematical model is first developed under specific conditions to display the construction and coupling of its individual components. It is then generalized to allow arbitrary projectile radius and Gaussian surface parameters, resulting in a generalized coupled mathematical model that relates projectile dynamics, granular resistance, geometric intersection, and particle flux quantity within a single mathematical framework.

Finally, the physical and chemical properties of granular materials are considered to provide a microscopic interpretation of the macroscopic model. In particular, the molecular and crystalline structures of silica-based granular materials are examined to describe the material properties that contribute to the total mechanical response of the granular medium. Together, the mathematical and physical descriptions provide a framework for studying the interaction between a solid projectile and a discrete granular medium without treating the granular material as an ordinary homogeneous fluid.

2 Mathematical Framework

2.1 Coordinate System and Arbitrary Geometric Boundaries

We define a frame of reference where the origin $(0, 0, 0)$ is fixed at the base center of the granular substance. The boundary of the granular pile is modeled as a three-dimensional continuous Gaussian surface:

$$z = h \cdot \exp\left[\frac{-(x^2 + y^2)}{\sigma^2}\right] \tag{1}$$

where "h" is defined as the height of the granular pile and "σ" is the horizontal length stretch along the x and y axes. The projectile is defined as a rigid sphere with the arbitrary radius (R) descending vertically along the z-axis with a time-dependent position, $z_c(t)$ or z_c:

$$x^2 + y^2 + (z - (z_c(t)))^2 = R^2 \tag{2}$$

where $\overrightarrow{c}(t)$ represents the position vector of the projectile's center, $\overrightarrow{c}(t) = (0, 0, z_c(t))$. These equations establish arbitrary geometric boundaries of the system.

2.2 Projectile Dynamics

The vertical motion of the projectile is modeled along the z-axis, with its center $z_c(t)$ or z_c. The velocity and acceleration of the projectile are $\frac{dz_c}{dt}$ and $\frac{d^2z_c}{dt^2}$. These can also be expressed as,

$$\frac{dz_c}{dt} = \dot{z_c} \tag{3}$$

for velocity, and

$$\frac{d^2z_c}{dt^2} = \ddot{z_c} \tag{4}$$

as acceleration.

In our model, we consider the projectile under the force of gravity alone, and with a force from interacting with granular substance. By modeling the Lagrangian and then applying the Euler-Lagrange equation, we obtain differential equations to model the dynamics of the system.

First, we consider the projectile under the influence of gravity alone.

$$T = \frac{1}{2}m_B\left(\frac{dz_c}{dt}\right)^2 = \frac{1}{2}m_B\dot{z_c}^2 \tag{5}$$

as the kinetic energy (T), and

$$U = m_B g z_c \tag{6}$$

as the potential energy (U). m_B represents the mass of the spherical projectile. We can then construct the Lagrangian for the gravitational force only, which is,

$$\mathcal{L}_g = T - U \tag{7}$$

or

$$\mathcal{L}_g(z_c, \dot{z_c}, t) = \frac{1}{2}m_B\dot{z_c}^2 - m_B g z_c \tag{8}$$

By applying the Euler-Lagrange equation,

$$\frac{d}{dt}\left[\frac{\partial \mathcal{L}_g}{\partial \dot{z_c}}\right] - \frac{\partial \mathcal{L}_g}{\partial z_c} = 0. \tag{9}$$

Evaluating the terms in the Euler-Lagrange equation gives,

$$\frac{\partial \mathcal{L}_g}{\partial \dot{z_c}} = m_B\dot{z_c} \tag{10}$$

so

$$\frac{d}{dt}\left[\frac{\partial \mathcal{L}_g}{\partial \dot{z_c}}\right] = m_B\ddot{z_c} \tag{11}$$

and

$$\frac{\partial \mathcal{L}_g}{\partial z_c} = -m_B g \tag{12}$$

therefore,

$$m_B \ddot{z}_c - (-m_B g) = 0 \tag{13}$$

giving us,

$$\ddot{z}_c = -g \tag{14}$$

which is the differential equation that represents the projectile's vertical motion under the influence of gravity alone. A solution to this differential equation, giving the baseline trajectory of our projectile, can be obtained by integrating twice along with the initial conditions, $z_c(0) = z_0$ and $\dot{z}_c(0) = v_0$.

$$\ddot{z}_c = -g \Longrightarrow \dot{z}_c = v_0 - gt \Longrightarrow z_c(t) = z_0 + v_0 t - \frac{1}{2} g t^2 \tag{15}$$

Furthermore, we must consider the projectile's granular interaction. Because the granular interaction is non-conservative, we can set the Euler-Lagrange equation equal to the generalized force Q,

$$\frac{d}{dt}\left(\frac{\partial \mathcal{L}_g}{\partial \dot{z}_c}\right) - \frac{\partial \mathcal{L}_g}{\partial z_c} = Q \tag{16}$$

where $Q = F_{granular}(t)$, and $F_{granular}(t)$ is the total time-dependent force exerted by the granular substance on the projectile, with the positive direction defined along the positive z-axis. The Euler-Lagrange equation therefore becomes,

$$\frac{d}{dt}\left(\frac{\partial \mathcal{L}_g}{\partial \dot{z}_c}\right) - \frac{\partial \mathcal{L}_g}{\partial z_c} = F_{granular}(t). \tag{17}$$

Because we know,

$$\frac{d}{dt}\left(\frac{\partial \mathcal{L}_g}{\partial \dot{z}_c}\right) = m_B \ddot{z}_c \tag{18}$$

and

$$\frac{\partial \mathcal{L}_g}{\partial z_c} = -m_B g. \tag{19}$$

Therefore,

$$m_B \ddot{z}_c - (-m_B g) = F_{granular}(t) \tag{20}$$

which simplifies to,

$$m_B \ddot{z}_c + m_B g = F_{granular}(t) \tag{21}$$

and finally

$$\ddot{z}_c = \frac{F_{granular}(t)}{m_B} - g. \tag{22}$$

A solution to this differential equation which gives us the trajectory of our projectile when interacting with the granular substance can be obtained by integrating twice, and having the initial conditions $z_c(0) = z_0$ and $\dot{z}_c(0) = v_0$. Starting from,

$$\ddot{z}_c = \frac{F_{granular}(t)}{m_B} - g. \tag{23}$$

integrating once,

$$\dot{z}_c(t) = v_0 + \int_0^t \left[\frac{F_{granular}(\tau)}{m_B} - g \right] d\tau \tag{24}$$

which can also be written as,

$$\dot{z}_c(t) = v_0 + \frac{1}{m_B} \int_0^t F_{granular}(\tau) d\tau - gt. \tag{25}$$

Integrating a second time gives,

$$z_c(t) = z_0 + \int_0^t \left[v_0 + \frac{1}{m_B} \int_0^\xi F_{granular}(\tau) d\tau - g\xi \right] d\xi \tag{26}$$

and simplifying again,

$$z_c(t) = z_0 + v_0 t - \frac{1}{2} g t^2 + \frac{1}{m_B} \int_0^t (t - \tau) F_{granular}(\tau) d\tau. \tag{27}$$

The $z_c(t) = z_0 + v_0 t - \frac{1}{2} g t^2$ segment represents the gravity-only trajectory, and the $\frac{1}{m_B} \int_0^t (t-\tau) F_{granular}(\tau) d\tau$ segment represents the granular contribution to the projectile's position as a function of time.

2.3 Discrete Granular System Approximation

Our original mechanical formulation was built around a discrete multi-body collision framework. Applying the law of conservation of linear momentum, the total initial momentum of the system must equal the final combined momentum of the projectile and the individual sand grains:

$$m_B \vec{v}_{B,i} = m_B \vec{v}_{B,f} + \sum_{j=1}^{N} m_j \vec{v}_{j,f} \tag{28}$$

where m_B is the mass of the projectile, $\vec{v}_{B,i}$ and $\vec{v}_{B,f}$ are its initial and final velocities, and m_j and $\vec{v}_{j,f}$ represent the individual mass and final velocity of the j-th discrete sand granule. But since a description of $N \approx 10^7$ independent grains is analytically unmanageable, we need to convert this discrete summation scheme into a continuum formulation.

2.4 Particle-Flux Density Field

So, we let N represent the total number of displaced grains. We construct a co-moving vector field $\vec{f} = \langle P, Q, R \rangle$ to represent the approximation of granular redistribution. To account for geometric spreading, we apply an inverse-square law relative to the moving center of the projectile:

$$\vec{f} = \left\langle \frac{N \cdot x}{r_{\text{ball}}^3}, \frac{N \cdot y}{r_{\text{ball}}^3}, \frac{N \cdot (z - z_c(t))}{r_{\text{ball}}^3} \right\rangle \tag{29}$$

where $r_{\text{ball}} = \sqrt{x^2 + y^2 + (z - z_c(t))^2}$.

The inverse square law is chosen to model the geometric spreading of displaced granules away from the impact region, assuming that the intensity of the displacement decreases proportionally to $\frac{1}{r^2}$ as the granules become more dispersed. We can show that $\nabla \cdot \vec{f} = 0$ for all points where $r_{\text{ball}} > 0$ by taking the divergence of our vector field. The divergence is,

$$\nabla \cdot \vec{f} = N \left[\frac{\partial}{\partial x} \left(\frac{x}{r_{ball}^3} \right) + \frac{\partial}{\partial y} \left(\frac{y}{r_{ball}^3} \right) + \frac{\partial}{\partial z} \left(\frac{z - z_c(t)}{r_{ball}^3} \right) \right]. \tag{30}$$

The three partial derivatives are,

$$\frac{\partial}{\partial x} \left(\frac{x}{r_{ball}^3} \right) = \frac{1}{r_{ball}^3} - \frac{3x^2}{r_{ball}^5}, \tag{31}$$

$$\frac{\partial}{\partial y} \left(\frac{y}{r_{ball}^3} \right) = \frac{1}{r_{ball}^3} - \frac{3y^2}{r_{ball}^5}, \tag{32}$$

and

$$\frac{\partial}{\partial z} \left(\frac{z - z_c(t)}{r_{ball}^3} \right) = \frac{1}{r_{ball}^3} - \frac{3(z - z_c(t))^2}{r_{ball}^5}. \tag{33}$$

So,

$$\nabla \cdot \vec{f} = N \left[\frac{3}{r_{ball}^3} - \frac{3\left[x^2 + y^2 + (z - z_c(t))^2\right]}{r_{ball}^5} \right]. \tag{34}$$

Since,

$$x^2 + y^2 + (z - z_c(t))^2 = r_{ball}^2, \tag{35}$$

we get

$$\nabla \cdot \vec{f} = N \left[\frac{3}{r_{ball}^3} - \frac{3r_{ball}^2}{r_{ball}^5} \right] = 0. \tag{36}$$

Thus, $\nabla \cdot \vec{f} = 0$ for all $r_{ball}0$.

The particle flux density field $\vec{f}$ is constructed by separating the system into its geometric magnitude and its unit directional vector. We defined the scalar intensity to obey a standard three-dimensional geometric attenuation (inverse-square law) scaled by the total grain count N:

$$\text{Magnitude} = \frac{N}{r_{\text{ball}}^2} \tag{37}$$

The sand granules are pushed radially outward from the moving impact center, creating a unit direction vector $\hat{u}$:

$$\hat{u} = \frac{\vec{r}_{\text{local}}}{r_{\text{ball}}} = \left\langle \frac{x}{r_{\text{ball}}}, \frac{y}{r_{\text{ball}}}, \frac{z - z_c(t)}{r_{\text{ball}}} \right\rangle \tag{38}$$

Multiplying the scalar magnitude by the directional unit vector establishes the final continuous field representation:

$$\vec{f} = (\text{Magnitude}) \times \hat{u} = \left(\frac{N}{r_{\text{ball}}^2}\right)\left(\frac{\vec{r}_{\text{local}}}{r_{\text{ball}}}\right) = \frac{N\vec{r}_{\text{local}}}{r_{\text{ball}}^3} \tag{39}$$

This algebraic expansion justifies the r_{ball}^3 term appearing in the Cartesian denominators.

2.5 Model Evolution and Domain Refinement

The volume integration with a pure continuum about the origin generates a singularity at $r_{\text{ball}} = 0$. Since granular material cannot exist inside the body of a solid projectile, we have to limit the integration volume $V(t)$ to a physically realizable domain. We define $V(t) =$ the bounded volume enclosed by $S_G(t) \cup S_B(t)$ where $S_G(t)$ is the relevant Gaussian surface patch and $S_B(t)$ is the submerged spherical surface patch. Their common boundary is the intersection curve $C(t)$:

$$\partial V(t) = S_G(t) \cup S_B(t), \quad S_G(t) \cap S_B(t) = C(t) \tag{40}$$

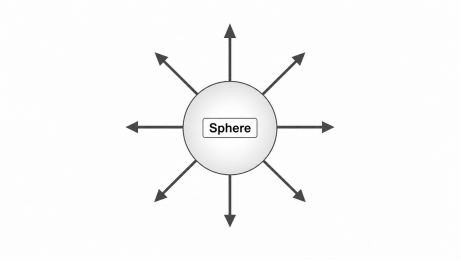


Figure 1: Two-Dimensional diagram of the radially outward particle flux vector field $\vec{f}$

radiating from the projectile boundary

The circular structure of the vector field is based on the observed outward displacement of granular material following the projectile impact. Although the field representation displays vectors extending in all radial directions around the projectile, the boundary inequalities defining $V(t)$ restrict the physically relevant region to the portion occupied by the granular heap. Hence the inequalities $(z \leq h \cdot \exp\left[\frac{-(x^2+y^2)}{\sigma^2}\right])$ and $z \geq 0$ serve as mathematical boundaries in $V(t)$ defining the physically applicable portion.

2.6 Reduction via the Divergence Theorem

Having defined $V(t)$ as the physically applicable integration domain as well as the divergence-free particle-flux density field $\vec{f}$, we can apply the Divergence

Theorem to relate the volume integral of the divergence to the net flux through the boundary of the granular region. The boundary $\partial V(t)$ consists of the Gaussian surface $S_{Gaussian}$ and the spherical projectile boundary S_{Ball}.

$$\iiint_{V(t)} (\nabla \cdot \vec{f})\, dV = \iint_{\partial V(t)} \vec{f} \cdot \hat{n} dS = 0. \tag{41}$$

Because $\partial V(t) = S_G(t) \cup S_B(t)$, this becomes

$$\iint_{S_G(t)} \vec{f} \cdot \hat{n}_G dS + \iint_{S_B(t)} \vec{f} \cdot \hat{n}_B dS = 0 \tag{42}$$

Therefore, $\Phi_G(t) = -\Phi_B(t)$. Now, by decomposing the boundary $\partial V(t)$, the net flux can be expressed as,

$$\iint_{\partial V(t)} \vec{f} \cdot \hat{n} dS = \iint_{S_{Gaussian}} \vec{f} \cdot \hat{n}_{Gaussian} dS - \iint_{S_{Ball}} \vec{f} \cdot \hat{n}_{Ball} dS. \tag{43}$$

Since $\iint_{\partial V(t)} \vec{f} \cdot \hat{n} dS = 0$,

$$\iint_{S_{Gaussian}} \vec{f} \cdot \hat{n}_{Gaussian} dS = \iint_{S_{Ball}} \vec{f} \cdot \hat{n}_{Ball} dS \tag{44}$$

Here, $\hat{n}_{Gaussian}$ denotes the outward normal from the granular region, while $\hat{n}_{Ball}$ denotes the outward normal from the projectile. Because the spherical boundary is an inner boundary of V(t), its outward normal relative to $V(t)$ is opposite to $\hat{n}_{Ball}$, producing the negative sign in the equation, $\hat{n}_{Ball,V} = -\hat{n}_{Ball}$.

Because $\nabla \cdot \overrightarrow{f} = 0$ within the open sand matrix, the volume integral simplifies, and the result is a flux-balance relation where the escaping flux through the surface equals the flux entering the granular region through the projectile boundary. Re-arranging the terms gives the resulting flux-balance relation, showing that the outward flux through the Gaussian surface equals the flux entering the granular region through the projectile boundary.

$$\iint_{S_{Gaussian}} \vec{f} \cdot \hat{n}_{Gaussian} dS = \iint_{S_{Ball}} \vec{f} \cdot \hat{n}_{Ball} dS. \tag{45}$$

3 Mathematical Analysis

3.1 Analysis Bounds and Preliminaries

To evaluate the mathematical model under a specific set of conditions, we choose the following parameters. For the simulated granular heap, we set $\sigma^2 = 1$ and $h = 1$, giving

$$z = e^{-(x^2+y^2)} \tag{46}$$

as the surface of the granular pile. We also set the projectile radius to $R = 1$, giving

$$x^2 + y^2 + (z - z_c(t))^2 = 1, \tag{47}$$

as the projectile boundary. Therefore, on S_{Ball},

$$r_{\text{ball}} = \sqrt{x^2 + y^2 + (z - z_c(t))^2} = 1. \tag{48}$$

To calculate the flux of our system through the spherical projectile boundary, we have the particle-flux density field.

$$\vec{f} = \left\langle \frac{Nx}{r_{\text{ball}}^3}, \frac{Ny}{r_{\text{ball}}^3}, \frac{N(z - z_c(t))}{r_{\text{ball}}^3} \right\rangle \tag{49}$$

Since $r_{Ball} = 1$ on S_{Ball}, the field simplifies when restricted to this surface.

$$\vec{f}\Big|_{S_{\text{Ball}}} = \langle N \cdot x, N \cdot y, N \cdot (z - z_c(t)) \rangle \,, \tag{50}$$

because $r_{ball}^3 = 1^3 = 1$ on S_{Ball}.

Because the Gaussian and projectile boundary fluxes are equal in magnitude, $\iint_{S_{Gaussian}} \vec{f} \cdot \hat{n}_{Gaussian} dS = \iint_{S_{Ball}} \vec{f} \cdot \hat{n}_{Ball} dS$, the projectile boundary may be used to evaluate the corresponding flux balance. Since only the portion of the projectile boundary interacting with the granular material contributes to the simulated collision, we define,

$$\Psi_{Ball}(t) = \iint_{S_{sub}(t)} \vec{f} \cdot \hat{n}_{Ball} dS. \tag{51}$$

The outward unit normal vector to the spherical projectile boundary is given by

$$\hat{n}_{Ball} = \langle x, y, z - z_c(t) \rangle \,. \tag{52}$$

Since the projectile has unit radius, the magnitude of this vector on S_{Ball} is

$$\| \langle x, y, z - z_c(t) \rangle \| = \sqrt{x^2 + y^2 + (z - z_c(t))^2} = 1. \tag{53}$$

Thus, $\hat{n}_{Ball}$ is a unit outward normal on S_{Ball}. Using the outward unit normal vector, we evaluate the flux density $\vec{f} \cdot \hat{n}_{Ball}$.

$$\vec{f} \cdot \hat{n}_{Ball} = \langle N \cdot x, N \cdot y, N \cdot (z - z_c(t)) \rangle \cdot \langle x, y, z - z_c(t) \rangle \,, \tag{54}$$

giving us,

$$\vec{f} \cdot \hat{n}_{Ball} = N \left[x^2 + y^2 + (z - z_c(t))^2 \right]. \tag{55}$$

Applying the spherical boundary condition,

$$x^2 + y^2 + (z - (z_c(t)))^2 = 1, \tag{56}$$

gives

$$\vec{f} \cdot \hat{n}_{Ball} = N. \tag{57}$$

Thus, the flux calculation reduces to evaluating the surface integral of the constant flux density, N, over the portion of the projectile boundary interacting with the granular material.

$$\Psi_{Ball}(t) = \iint_{S_{sub}(t)} N dS \tag{58}$$

3.2 Evaluating the Mathematical Model

We have defined the surface integral we need to solve as,

$$\Psi_{Ball}(t) = \iint_{S_{sub}(t)} N dS. \tag{59}$$

Transforming to local spherical coordinates where

$$x = \sin\phi\cos\theta, \tag{60}$$

$$y = \sin\phi\sin\theta, \tag{61}$$

and

$$z = z_c(t) - \cos\phi. \tag{62}$$

The surface-area element is obtained from the parametrization of the spherical surface. The parametrization of the unit-radius spherical projectile surface is

$$\vec{r}(\phi,\theta,t) = \langle \sin\phi\cos\theta, \sin\phi\sin\theta, z_c(t) - \cos\phi \rangle . \tag{63}$$

The tangent vectors to this parametrized surface are

$$\frac{\partial\vec{r}}{\partial\phi} = \langle \cos\phi\cos\theta, \cos\phi\sin\theta, \sin\phi \rangle \tag{64}$$

and

$$\frac{\partial\vec{r}}{\partial\theta} = \langle -\sin\phi\sin\theta, \sin\phi\cos\theta, 0 \rangle . \tag{65}$$

The surface-area element is obtained from the magnitude of their cross product:

$$dS = \left\| \frac{\partial\vec{r}}{\partial\phi} \times \frac{\partial\vec{r}}{\partial\theta} \right\| d\phi\, d\theta. \tag{66}$$

Evaluating the cross product gives

$$\frac{\partial\vec{r}}{\partial\phi} \times \frac{\partial\vec{r}}{\partial\theta} = \left\langle -\sin^2\phi\cos\theta, -\sin^2\phi\sin\theta, \sin\phi\cos\phi \right\rangle , \tag{67}$$

whose magnitude is

$$\left\| \frac{\partial\vec{r}}{\partial\phi} \times \frac{\partial\vec{r}}{\partial\theta} \right\| = \sin\phi. \tag{68}$$

Therefore, the surface-area element on the unit sphere is $dS = \sin\phi d\phi d\theta$. The submerged region of the spherical projectile is determined by its intersection with the Gaussian granular surface. We define $\phi_{sub}(t)$ as the polar angle that determines the boundary of the portion of S_{Ball} submerged within the granular region at time t. The limiting angle $\phi_{sub}(t)$ can be derived from,

$$x^2 + y^2 = \sin^2\phi(\sin^2\theta + \cos^2\theta), \tag{69}$$

where $\sin^2\theta + \cos^2\theta = 1$, so the Gaussian surface becomes

$$z = e^{-\sin^2\phi}. \tag{70}$$

From the sphere we have, $z = z_c(t) + \cos\phi$, and setting it equal to the Gaussian surface,

$$e^{-\sin^2\phi} = z_c(t) - \cos\phi \tag{71}$$

or equivalently,

$$e^{-\sin^2\phi} - z_c(t) + \cos\phi = 0. \tag{72}$$

$\phi_{sub}(t)$ is determined implicitly by $e^{-\sin^2\phi_{sub}(t)} - z_c(t) + \cos\phi_{sub}(t) = 0$. The solution of this intersection equation defines the limiting polar angle $\phi_{sub}(t)$, so that the submerged region is described by $0 \leq \phi \leq \phi_{sub}(t)$.

$$\Psi_{Ball}(t) = \int_0^{2\pi}\int_0^{\phi_{sub}(t)} N\sin\phi d\phi d\theta. \tag{73}$$

Then,

$$\int_0^{\phi_{sub}(t)} N\sin\phi d\phi = N(1 - \cos\phi_{sub}(t)), \tag{74}$$

so

$$\int_0^{2\pi} N(1 - \cos\phi_{sub}(t))d\theta = 2\pi N(1 - \cos\phi_{sub}(t)). \tag{75}$$

Therefore, the total particle flux through the submerged portion of the projectile boundary is,

$$\Psi_{Ball}(t) = 2\pi N[1 - \cos\phi_{sub}(t)]. \tag{76}$$

For the purpose of this mathematical simulation, the measurable variables are dimensionless. Hence, $R = 1$ and $h = 1$ represent the chosen length scale rather than physical lengths of one meter. The variable N denotes the total number of grains in our simulated granular system.

3.3 Coupling Projectile Dynamics and Particle Flux

From the previous sections, we have expressions for the modeled particle-flux quantity and the projectile's dynamics.

$$\Psi_{Ball}(t) = 2\pi N[1 - \cos\phi_{sub}(t)], \tag{77}$$

and

$$\ddot{z}_c = \frac{F_{granular}(t)}{m_B} - g. \tag{78}$$

We set,

$$\Gamma(z_c(t), \phi_{sub}(t)) = e^{-\sin^2 \phi_{sub}(t)} - z_c(t) + \cos \phi_{sub}(t) = 0. \tag{79}$$

The intersection condition is time-dependent because the projectile center $z_c(t)$ changes during the collision. Therefore, the limiting polar angle $\phi_{sub}(t)$ must also vary with time in order for the projectile surface to remain constrained to the granular boundary. Applying the chain rule and differentiating with respect to time gives,

$$\frac{d\Gamma}{dt} = \frac{\partial \Gamma}{\partial z_c}\dot{z}_c + \frac{\partial \Gamma}{\partial \phi_{sub}}\dot{\phi}_{sub} = 0 \tag{80}$$

where,

$$\frac{\partial \Gamma}{\partial z_c} = -1, \tag{81}$$

and

$$\frac{\partial \Gamma}{\partial \phi_{sub}} = -2 \sin \phi_{sub} \cos \phi_{sub} e^{-\sin^2 \phi_{sub}} - \sin \phi_{sub}, \tag{82}$$

so,

$$\frac{d\Gamma}{dt} = -\dot{z}_c + [-2 \sin \phi_{sub} \cos \phi_{sub} e^{-\sin^2 \phi_{sub}} - \sin \phi_{sub}]\dot{\phi}_{sub} = 0. \tag{83}$$

Isolating $\dot{\phi}_{sub}$,

$$\dot{\phi}_{sub} = -\frac{\dot{z}_c}{\sin \phi_{sub}(2 \cos \phi_{sub} e^{-\sin^2 \phi_{sub}} + 1)}. \tag{84}$$

This result shows that the rate of change of the submerged polar angle is determined by the instantaneous vertical velocity of the projectile and the local geometry of the Gaussian boundary. Thus, the geometric intersection is dynamically coupled to the projectile motion rather than being treated as a fixed geometric quantity. The modeled particle-flux quantity is,

$$\Psi_{Ball}(t) = 2\pi N[1 - \cos \phi_{sub}(t)]. \tag{85}$$

Because the modeled particle-flux quantity depends explicitly on $\phi_{sub}(t)$, its temporal evolution can be obtained by applying the chain rule. So differentiating with respect to time establishes a connection between the projectile velocity and the rate of change of the submerged boundary.

$$\frac{d\Psi_{Ball}}{dt} = 2\pi N \sin \phi_{sub} \dot{\phi}_{sub}. \tag{86}$$

Substituting $\dot{\phi}_{sub}$ gives,

$$\frac{d\Psi_{Ball}}{dt} = 2\pi N \sin \phi_{sub} \left[-\frac{\dot{z}_c}{\sin \phi_{sub}(2 \cos \phi_{sub} e^{-\sin^2 \phi_{sub}} + 1)} \right] \tag{87}$$

and simplifying,

$$\frac{d\Psi_{Ball}}{dt} = -\frac{2\pi N \dot{z}_c}{2\cos\phi_{sub} e^{-\sin^2\phi_{sub}} + 1}. \tag{88}$$

The resulting expression directly couples the projectile velocity to the rate of change of the modeled particle-flux quantity. As the projectile moves through the granular surface, its changing position modifies $\phi_{sub}(t)$, which in turn changes the submerged surface area and the modeled particle-flux quantity. Thus, the particle-flux evolution is coupled to both the projectile dynamics and the instantaneous geometric intersection with the granular surface. The projectile velocity itself depends on the granular resistance, which is modeled in the following subsection.

3.4 Modeling the Granular Interaction Force

We can use the quadratic drag equation to model our $F_{granular}$. The quadratic drag equation is $F_d = \frac{1}{2}\rho C_d A \nu^2$ where ρ represents the density of our sand, C_d represents the drag coefficient, ν^2 represents the square of the projectile speed, and A represents the submerged surface area. To approximate the granular resistance acting on the submerged portion of the projectile, we adopt an effective quadratic continuum resistance model in which we define the effective interaction area A_{eff} to be the submerged spherical surface area of the projectile. This choice differs from the conventional projected frontal area used in standard aerodynamic drag models; here, the submerged spherical surface area is adopted as an effective area to represent the distributed interaction between the projectile and granular medium. From the equation,

$$\Psi_{Ball}(t) = 2\pi N[1 - \cos\phi_{sub}(t)], \tag{89}$$

and because the simulation uses $R = 1$, the corresponding effective interaction area is therefore,

$$A_{eff}(t) = \int_0^{2\pi}\int_0^{\phi_{sub}} (1)^2 \sin\phi d\phi d\theta = 2\pi[1 - \cos\phi_{sub}(t)] \tag{90}$$

as a function of time. Putting it all together gives,

$$F_{granular}(t) = -\pi\rho C_d[1 - \cos\phi_{sub}(t)]\,|\dot{z}_c|\,\dot{z}_c, \tag{91}$$

where the negative sign ensures that the granular resistance opposes the direction of projectile motion, while $|\dot{z}_c|\,\dot{z}_c$ preserves the appropriate direction of the resistance for either sign of $\dot{z}_c$. Our projectile equation will now become,

$$\ddot{z}_c = -\frac{\pi\rho C_d}{m_B}[1 - \cos\phi_{sub}(t)]\,|\dot{z}_c|\,\dot{z}_c - g. \tag{92}$$

We solve a differential-algebraic system of equations with the initial conditions of, $z_c(0) = z_0$ and $\dot{z}_c(0) = v_0$ and algebraic part being $\Gamma(z_c, \phi_{sub}) =$

$e^{-\sin^2\phi_{sub}(t)} - z_c(t) + \cos\phi_{sub}(t) = 0$. $\Gamma(z_c, \phi_{sub})$ serves as the algebraic constraint because ϕ_{sub} is implicitly determined by the instantaneous projectile position $z_c(t)$, while simultaneously governing the granular resistance in the differential equation.

$$\begin{cases} \ddot{z}_c = -\frac{\pi\rho C_d}{m_B}[1-\cos\phi_{sub}(t)]\,|\dot{z}_c|\,\dot{z}_c - g \\ \Gamma(z_c,\phi_{sub}) = e^{-\sin^2\phi_{sub}(t)} - z_c(t) + \cos\phi_{sub}(t) = 0 \end{cases} \tag{93}$$

The differential-algebraic system determines ϕ_{sub}, which also determines the time-dependent particle flux as well as the projectile dynamics of our system.

$$\begin{cases} \ddot{z}_c = -\frac{\pi\rho C_d}{m_B}[1-\cos\phi_{sub}(t)]\,|\dot{z}_c|\,\dot{z}_c - g \\ \Gamma(z_c,\phi_{sub}) = e^{-\sin^2\phi_{sub}(t)} - z_c(t) + \cos\phi_{sub}(t) = 0 \\ \Psi_{Ball}(t) = 2\pi N[1-\cos\phi_{sub}(t)] \end{cases} \tag{94}$$

Together, these equations provide a coupled mathematical description of the projectile dynamics, granular resistance, geometric interaction, and particle flux.

4 Generalized Mathematical Model

4.1 Generalized Coupled Model

To generalize the projectile geometry from the Cartesian representation used previously, we introduce a spherical-coordinate parameterization of the projectile surface.

$$x = R\sin\phi\cos\theta, \tag{95}$$

$$y = R\sin\phi\sin\theta, \tag{96}$$

and

$$z = z_c - R\cos\phi. \tag{97}$$

To find the surface-area element we parameterize the arbitrary spherical surface which gives,

$$\vec{r}(\phi,\theta,t) = \langle R\sin\phi\cos\theta, R\sin\phi\sin\theta, z_c(t) - R\cos\phi\rangle\,. \tag{98}$$

The tangent vectors to this parameterized surface are

$$\frac{\partial\vec{r}}{\partial\phi} = \langle R\cos\phi\cos\theta, R\cos\phi\sin\theta, R\sin\phi\rangle \tag{99}$$

and

$$\frac{\partial\vec{r}}{\partial\theta} = \langle -R\sin\phi\sin\theta, R\sin\phi\cos\theta, 0\rangle\,. \tag{100}$$

Evaluating the cross product gives,

$$\frac{\partial\vec{r}}{\partial\phi}\times\frac{\partial\vec{r}}{\partial\theta} = \left\langle -R^2\sin^2\phi\cos\theta, -R^2\sin^2\phi\sin\theta, R^2\sin\phi\cos\phi\right\rangle \tag{101}$$

with a magnitude of

$$\left\| \frac{\partial \vec{r}}{\partial \phi} \times \frac{\partial \vec{r}}{\partial \theta} \right\| = R^2 \sin \phi. \tag{102}$$

Therefore the surface area element of the spherical projectile is $dS = R^2 \sin\phi d\phi d\theta$. Our vector field is $\vec{f} = \left\langle \frac{Nx}{r_{\text{ball}}^3}, \frac{Ny}{r_{\text{ball}}^3}, \frac{N(z-z_c(t))}{r_{\text{ball}}^3} \right\rangle$ and an outward radial normal vector to the spherical projectile is given by, $\vec{n}_{Ball} = \frac{1}{R} \langle x, y, z - z_c(t) \rangle$, with magnitude R, giving us our flux density.

$$\vec{f} \cdot \vec{n}_{Ball} = \left\langle \frac{Nx}{r_{ball}^3}, \frac{Ny}{r_{ball}^3}, \frac{N(z-z_c(t))}{r_{ball}^3} \right\rangle \cdot \frac{1}{R} \langle x, y, z - z_c(t) \rangle = \frac{N}{R r_{ball}} \tag{103}$$

On the spherical projectile, $R = r_{ball}$, so this becomes $\frac{N}{R^2}$. Using this surface area element as well as our bounds $0 \leq \phi \leq \phi_{sub}(t)$ and $0 \leq \theta \leq 2\pi$, our surface integral becomes,

$$\Psi_{Ball,Generalized}(t) = \iint \vec{f} \cdot \vec{n}_{Ball} dS = \int_0^{2\pi} \int_0^{\phi_{sub}(t)} \frac{N}{R^2} R^2 \sin\phi d\phi d\theta. \tag{104}$$

Evaluating gives,

$$\Psi_{Ball,Generalized}(t) = 2\pi N(1 - \cos\phi_{sub}(t)). \tag{105}$$

A generalized version of our geometric interaction between the projectile and the granular medium $\Gamma(z_c(t), \phi_{sub}(t)$ is obtained by setting the Gaussian boundary equal to the projectiles position on the z-axis relevant to time. Ultimately giving us,

$$\Gamma_{Generalized}(z_c(t), \phi_{sub}(t)) = h \cdot \exp\left[-\frac{R^2 \sin^2 \phi_{sub}(t)}{\sigma^2} \right] - z_c(t) + R\cos\phi_{sub}(t) = 0 \tag{106}$$

Differentiating with respect to time and applying the multi variable chain rule gives,

$$\frac{d\Gamma_{Generalized}}{dt} = \frac{\partial \Gamma_{Generalized}}{\partial z_c} \dot{z}_c + \frac{\partial \Gamma_{Generalized}}{\partial \phi_{sub}} \dot{\phi}_{sub} = 0 \tag{107}$$

where

$$\frac{\partial \Gamma_{Generalized}}{\partial z_c} = -1, \tag{108}$$

and

$$\frac{\partial \Gamma_{Generalized}}{\partial \phi_{sub}} = -\frac{2hR^2}{\sigma^2} \sin\phi_{sub} \cos\phi_{sub} \exp\left[\frac{-R^2 \sin^2 \phi_{sub}}{\sigma^2} \right] - R\sin\phi_{sub}. \tag{109}$$

So,

$$\frac{d\Gamma_{Generalized}}{dt} = -\dot{z}_c + \left[-\frac{2hR^2}{\sigma^2} \sin\phi_{sub} \cos\phi_{sub} \exp\left[\frac{-R^2 \sin^2 \phi_{sub}}{\sigma^2} \right] - R\sin\phi_{sub} \right] \dot{\phi}_{sub} = 0 \tag{110}$$

Isolating $\dot{\phi}_{sub}$ provides the generalized evolution equation for the submerged polar angle. The rate of change of $\phi_{sub}(t)$ is determined by the instantaneous vertical velocity of the projectile and the local geometry of the Gaussian boundary:

$$\dot{\phi}_{sub} = -\frac{\dot{z}_c}{\frac{2hR^2}{\sigma^2}\sin\phi_{sub}\cos\phi_{sub}\exp\left[\frac{-R^2\sin^2\phi_{sub}}{\sigma^2}\right] + R\sin\phi_{sub}} \tag{111}$$

The submerged portion of the spherical projectile provides the effective interaction area used to approximate the distributed granular resistance. Since the surface area of a spherical cap bounded by $\phi_{sub}(t)$ is determined by its radius and limiting polar angle, the generalized effective interaction area is

$$A_{eff}(t) = \int_0^{2\pi}\int_0^{\phi_{sub}} R^2\sin\phi d\phi d\theta = 2\pi R^2[1-\cos\phi_{sub}(t)] \tag{112}$$

Using this effective interaction area in the quadratic continuum drag approximation gives the generalized granular resistance:

$$F_{granular}(t) = -\pi\rho C_d R^2[1-\cos\phi_{sub}(t)]\,|\dot{z}_c|\,\dot{z}_c \tag{113}$$

The negative sign ensures that the granular resistance opposes the instantaneous direction of projectile motion, while the factor $|\dot{z}_c|\,\dot{z}_c$ preserves the appropriate direction of the resistance for either sign of $\dot{z}_c$. Substituting this generalized granular force into the projectile equation of motion gives

$$\ddot{z}_c = \frac{-\pi\rho C_d R^2}{m_B}[1-\cos\phi_{sub}(t)]\,|\dot{z}_c|\,\dot{z}_c - g. \tag{114}$$

The projectile dynamics and geometric intersection are therefore coupled through both $z_c(t)$ and $\phi_{sub}(t)$. The projectile position and velocity determine the instantaneous state of the projectile, while the algebraic intersection constraint determines the corresponding submerged polar angle. This produces the following differential-algebraic system, together with the initial conditions $z_c(0) = z_0$ and $\dot{z}_c(0) = v_0$:

$$\begin{cases} \ddot{z}_c = \frac{-\pi\rho C_d R^2}{m_B}[1-\cos\phi_{sub}(t)]\,|\dot{z}_c|\,\dot{z}_c - g \\ \Gamma_{Generalized}(z_c(t),\phi_{sub}(t)) = h\cdot\exp\left[-\frac{R^2\sin^2\phi_{sub}(t)}{\sigma^2}\right] - z_c(t) + R\cos\phi_{sub}(t) = 0 \end{cases} \tag{115}$$

The coupled evolution of the projectile position, projectile velocity, and submerged geometry is represented by this formulation for arbitrary values of the projectile radius and the parameters defining the Gaussian surface. The algebraic condition ensures the geometric intersection of the projectile with the granular boundary at all times. The differential equation determines the projectile dynamics under gravity and the modeled granular resistance. The generalized particle-flux quantity can then be recovered from the coupled solution. We refer to the resulting expression as the master equation because it maps

the coupled projectile and geometric dynamics onto the time evolution of the modeled particle-flux quantity. Starting from

$$\Psi_{Ball,Generalized}(t) = 2\pi N(1 - \cos\phi_{sub}(t)), \tag{116}$$

then differentiating with respect to time gives,

$$\frac{d\Psi_{Ball,Generalized}}{dt} = 2\pi N \sin\phi_{sub}\dot{\phi}_{sub}. \tag{117}$$

Then substituting the generalized $\dot{\phi}_{sub}(t)$,

$$\frac{d\Psi_{Ball,Generalized}}{dt} = 2\pi N \sin\phi_{sub}\left(-\frac{\dot{z}_c}{\frac{2hR^2}{\sigma^2}\sin\phi_{sub}\cos\phi_{sub}\exp\left[\frac{-R^2\sin^2\phi_{sub}}{\sigma^2}\right] + R\sin\phi_{sub}}\right). \tag{118}$$

Canceling the common factor of $\sin\phi_{sub}$ and factoring out R from the denominator gives the final generalized expression:

$$\frac{d\Psi_{Ball,Generalized}}{dt} = -\frac{2\pi N}{R}\left(\frac{\dot{z}_c}{1 + \frac{2hR}{\sigma^2}\cos\phi_{sub}\exp\left[\frac{-R^2\sin^2\phi_{sub}}{\sigma^2}\right]}\right). \tag{119}$$

This final expression connects the modeled particle-flux evolution directly to the generalized projectile dynamics and the instantaneous geometry of the granular boundary. Consequently, the complete generalized model consists of the projectile parameterization, surface-flux formulation, geometric intersection constraint, granular resistance model, projectile equation of motion, and master equation for the modeled particle-flux quantity.

4.2 Implicit Determination of the Submerged Angle

The submerged polar angle $\phi_{sub}(t)$ is determined implicitly by the intersection between the projectile surface and the granular boundary. Substituting the spherical parameterization into the generalized Gaussian boundary yields the constraint

$$h \cdot \exp\left[-\frac{R^2\sin^2\phi}{\sigma^2}\right] - z_c(t) + R\cos\phi = 0. \tag{120}$$

This equation is transcendental in $\phi_{sub}(t)$ and does not admit a solution in elementary functions. Consequently, $\phi_{sub}(t)$ is treated as an implicitly defined function of the projectile position $z_c(t)$ rather than being expressed explicitly. For notational convenience, define

$$\Gamma_{Generalized}(z_c, \phi) = h \cdot \exp\left[-\frac{R^2\sin^2\phi}{\sigma^2}\right] - z_c(t) + R\cos\phi = 0 \tag{121}$$

such that the geometric constraint is

$$\Gamma_{Generalized}(z_c, \phi_{sub}(t)) = 0. \tag{122}$$

The governing equations derived previously therefore remain valid with $\phi_{sub}(t)$ understood as the physically admissible solution of this implicit constraint. Numerical root-finding methods may be employed to evaluate $\phi_{sub}(t)$ for specific parameter values, but such computation is not required for the analytical formulation developed in this work.

5 Chemical Physics of Granular Locking

In order to understand the limitations and discrepancies within our continuum model, it is necessary to explore the material parameters at the microscopic level that dictate the dynamics of the granular system on a macroscopic scale. Granular matter can exhibit markedly different mechanical states, transitioning between fluid-like flow and solid-like load-bearing behaviour under changes in stress and packing conditions.

5.1 Microscopic Lattice Architecture of α-Quartz

The principal component of many common sands is silica (SiO_2) , which commonly occurs in the α-quartz crystalline form. At the microscopic scale, sand granules are not composed of freely separated molecules, but rather form continuous covalent network solids. The crystal structure comprises SiO_4 silicon-oxygen tetrahedral units sharing corners periodically in three dimensional space [1]. As silicon is able to create four bonds with neighboring atoms, it creates a bond of

$$|\overrightarrow{r_O} - \overrightarrow{r_{Si}}| \approx 1.61\mathring{A}$$

with each of its four neighboring oxygen atoms [1]. As this lattice is in the shape of a tetrahedron, its bond angle is

$$\theta = \cos^{-1}(-\frac{1}{3}) = 109.47^\circ \quad [1].$$

The tetrahedral bonding geometry corresponds to a low-energy configuration of the crystal structure and contributes to its mechanical stiffness. The other parameter that can be used to characterize the resistance to elastic deformation of quartz is the Young's modulus. The Young's modulus of quartz is approximately $E \approx 70 - 100 \quad GPa.$ depending on crystallographic direction [2]. High elastic modulus means that the strain,

$$\varepsilon = \frac{\sigma}{E},$$

will be relatively low for impact loads [3]. Since the elastic deformation of an individual grain is small relative to the translational and rotational motion of the grain as a whole, each grain can be approximated as a rigid body [4]. As a result, a substantial portion of the impact energy is transferred through grain contacts, friction, and the motion of the grains themselves [5].

Since the Si–O covalent bonds have extremely high bond energies and the quartz structure has a high elastic modulus, the grains can often be approximated as mechanically rigid under the impact conditions considered here. Under the impact conditions considered here, the elastic deformation in an individual grain is extremely small relative to the translation and movement of the grains themselves. Thus, under the impact conditions considered here, only a relatively small fraction of the projectile's kinetic energy is expected to be stored temporarily as elastic deformation within individual quartz grains. A substantial portion of the impact energy is therefore expected to be transferred through contact forces between grains, friction, and the translational and rotational motion of the grains themselves [5].

5.2 Macroscopic Jamming Transitions

The sudden increase in resistance experienced by the projectile can be interpreted in terms of a granular jamming transition [6]. Unlike a continuum fluid, a densely packed granular medium cannot sustain macroscopic deformation without rearrangement of its grains. Such rearrangement generally requires grains to roll, slide, or translate relative to their neighbors, increasing the available interstitial volume. This phenomenon is known as Reynolds dilatancy [6].

During sufficiently rapid impact, the imposed deformation can occur faster than the granular medium can rearrange uniformly [7]. The grains therefore have insufficient time to reorganize uniformly, producing transient force chains and localized regions of high stress [8]. The resulting increase in mechanical resistance provides a microscopic interpretation of the effective granular force introduced in the continuum model.

6 Conclusion

This work developed a continuum mathematical framework for describing particle flux and projectile dynamics during granular impact. By representing the granular region with an arbitrary geometric boundary and coupling the resulting flux formulation to projectile dynamics, the model provides a generalized description of the interaction between a projectile and a granular medium. The framework was extended to arbitrary projectile radius and granular-heap geometry, while a microscopic description of quartz and granular jamming was used to provide physical context for the modeled resistance. The resulting formulation provides a mathematical basis for analyzing granular impact without requiring a closed-form solution for the submerged boundary.

7 References

Disclaimer, AI was used in conveying some parts of the paper. These parts include, the references, editing grammatical errors, wording, and the image

displayed on page 7.

[1] J. P. Sutter, J. Pittard, J. Filik, and A. Q. R. Baron, "Calculating temperature-dependent X-ray structure factors of -quartz with an extensible Python 3 package," *Journal of Applied Crystallography*, vol. 55, no. 4, pp. 1011–1028, 2022. doi: 10.1107/S1600576722005945.

[2] P. R. Heyliger, H. Ledbetter, and S. A. Kim, "Elastic constants of natural quartz," *The Journal of the Acoustical Society of America*, vol. 114, no. 2, pp. 644–650, 2003. doi: 10.1121/1.1593063.

[3] Massachusetts Institute of Technology, "Mechanics of Materials: Elasticity," *MIT OpenCourseWare*.

[4] K. L. Johnson, *Contact Mechanics*. Cambridge, U.K.: Cambridge University Press, 1985.

[5] A. H. Clark, L. Kondic, and R. P. Behringer, "Particle scale dynamics in granular impact," *Physical Review Letters*, vol. 109, no. 23, 238302, 2012. doi: 10.1103/PhysRevLett.109.238302.

[6] R. P. Behringer and B. Chakraborty, "The physics of jamming for granular materials: a review," *Reports on Progress in Physics*, vol. 82, no. 1, 012601, 2019. doi: 10.1088/1361-6633/aadc3c.

[7] A. H. Clark, A. J. Petersen, L. Kondic, and R. P. Behringer, "Nonlinear force propagation during granular impact," *Physical Review Letters*, vol. 114, no. 14, 144502, 2015. doi: 10.1103/PhysRevLett.114.144502.

[8] R. P. Behringer, "Jamming in granular materials," *Comptes Rendus Physique*, vol. 16, no. 1, pp. 10–25, 2015. doi: 10.1016/j.crhy.2015.02.001.